Nationaal Lucht- en Ruimtevaartlaboratorium
National Aerospace Laboratory NLR

NLR-TP-2002-004

Aerodynamic and aero-acoustic effects of flap tip fences

J.W. Slooff, W.B. de Wolf, H.M.M. van der Wal and
J.E.J. Maseland

This report is based on a presentation held at the 40th AIAA Aerospace Sciences Meeting & Exhibition, at Reno, NV on 14-17 January 2002.

Customer:	National Aerospace Laboratory NLR
Working Plan number:	A.1.A.1
Owner:	National Aerospace Laboratory NLR
Division:	Fluid Dynamics
Distribution:	Unlimited
Classification title:	Unclassified
	December 2002

Abstract

The application of winglet or end-plate type devices to the tips of the trailing-edge flap of a wing has, for some time, been suggested as a (potential) means for improving the aerodynamic efficiency during take-off/climb and for decreasing the airframe noise of transport aircraft in the approach/landing configuration. A third aspect of the application of such devices is their possible effect on the wake vortex characteristics.
In this paper the main results and conclusions are presented of exploratory CFD simulations and low-speed wind tunnel tests on a half model of a civil transport type of aircraft configuration with trailing-edge flaps extended and with (and without) winglet type "fences" attached to the main wing at the position of the outboard tip of the trailing-edge flap. Both take-off/climb and approach/landing flap settings were tested.
The main results of the investigation are that the application of flap tip fences may lead to:

- a substantial (up to 7 dB) reduction of the sound power level of the flap tip noise source in the approach/landing configuration (about equal for the lower and the upper + lower fence configurations)
- a (small) improvement of L/D and C_{Lmax} in take-off/climb of up to 1% (lower fence only)
- possibly a small reduction of a few percent of the strength of the wake vortex from the flap tip region

List of symbols

b	(full) wing span	
c	local wing chord	
C_D	drag coefficient	
C_L	wing lift coefficient	
D_i	induced drag	
L_W	sound power level	re 10^{-12} W
P	Sound Power	Watt
v	velocity in y-direction	
w	velocity in z-direction	
x	axial coordinate	
y	spanwise coordinate	
z	coordinate perpendicular to x, y plane	
Y	vertical tunnel coordinate	
Z	lateral tunnel coordinate	
α	wing angle of attack	
α_i	induced angle of attack	
Γ	circulation	
η	y/(b/2)	
ω_x	streamwise velocity	

List of abbreviations

DNW	Duits-Nederlandse Windtunnel (German-Dutch Wind Tunnels)
FTF	Flap Tip Fence
HST	High Speed Tunnel (of DNW)
LLF	Large Low Speed Facility (of DNW)
LST	Low Speed Tunnel (of DNW)
NACA	National Advisory Committee for Aeronautics
NLR	Nationaal Lucht- en Ruimtevaartlaboratorium (National Aerospace Laboratory)
PIV	Particle Image Velocimetry

Contents

(29 pages in total)

1 Introduction

It has, for some time, been suggested that the application of end-plate or winglet type devices to the tips of the trailing-edge flaps of (transport) aircraft (fig.1) could be beneficial for the aerodynamic and acoustic characteristics:

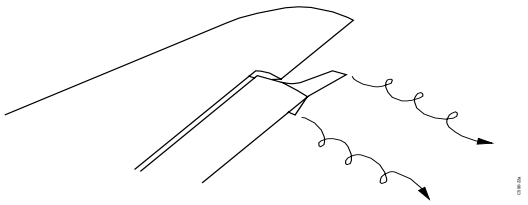

Fig. 1 Sketch illustrating the concept of winglet type flap tip devices

- In refs. 1 and 2 it was suggested that the addition of winglet type devices to the tip of a trailing-edge flap of an aircraft (fig.1) might:
  - increase L/D through a reduction of induced drag (important for take-off and second-segment climb)
  - reduce airframe noise generated by the flap tip (particularly important for the approach/landing configuration)
  - improve the wake vortex characteristics
  - lead to a (small) increase in maximum lift
- For a simple, straight wing, of aspect ratio 5.3 with a 30%-span flap an increase in L/D, due to the addition of winglet type devices to the tips of the flap, of up to 2.5% was reported as early as 1987 [3]
- In ref. 4 a noise reduction of up to 5 dB (sound pressure level), due to the addition of simple, flat end-plates to the flap tips, is reported from an acoustic wind tunnel test on a DC-10 model

This led NLR to initiate, in 1998, a (small) exploratory research project to (further) investigate the potential of winglet type flap tip devices for improvement of the aerodynamic and aero-acoustic properties of transport aircraft. As a first step a computational study was performed, using an 'unstructured' Euler code, of the aerodynamic consequences of adding 'fence'-like devices to the wing of a large, low-speed aircraft (wing plus fuselage) configuration, the geometry of which was provided by Deutsche Airbus (Bremen). For reasons to be addressed in section 2 of this paper, these 'fences' were attached to the main wing, but at the spanwise position of the outboard tip of the trailing-edge flap, rather than to the flap tips themselves (fig. 2).

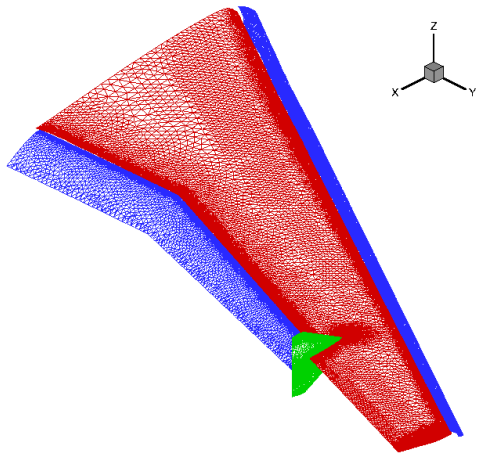

Fig. 2 Example of 'fence'-type flap tip device, attached to the main wing of an aircraft

As a second step wind tunnel tests were envisaged on a model of Deutsche Airbus in the LLF of DNW.

During this computational study[5] two problems were encountered. The first problem was an unexpectedly high aerodynamic loading (side force) of the fences, suggesting a substantial risk of leading-edge vortex flow type separation on the fences. It was concluded that this was associated with the high loading of the main wing in combination with the (30 degrees) sweep angle of the wing and that a reduction of the loading on the (over-active) fences would require a change of the (lateral) incidence angle of the fences.

The second problem was that the available post-processing routine for the determination of induced drag through Trefftz-plane analysis was not capable to deal with the rather complex wing plus flap plus slat plus fuselage configuration. Consequently a new post-processing routine for induced drag had to be written. Application of this new routine suggested a potential for a reduction of induced drag of about 10 'drag counts', that is about 1% of the total drag, for the take-off/climb configuration[5].

As a consequence of these problems the available time slot in the DNW-LLF for the wind tunnel tests could not be met. Instead, it was decided to perform wind tunnel tests in the DNW-LST on a half-model of a (different) transport-type aircraft configuration that was available at NLR. This paper presents the main results and conclusions of these wind tunnel tests.

2 Flap tip fence design considerations

Establishing guidelines for the (conceptual) design of flap tip devices intended for induced drag and noise reductions requires understanding of the aerodynamic and aero-acoustic mechanisms of wings with deployed high-lift devices:

2.1 Aerodynamics

Wings are equipped with high-lift devices (trailing edge flaps and leading-edge slats) to improve performance during take-off, climb, approach and landing. The high-lift devices provide additional lift through[6]:

- an (effectively) increased airfoil camber by flap/slat deflection
- favourable aerodynamic interaction (reduction of pressure gradients) between main airfoil, slat and flap
- re-energizing or 'dumping' (removing) low energy boundary layers.
- an increase of the effective wing area

For this study the aerodynamic and aero-acoustic mechanisms involved with trailing edge flaps are of particular interest.

Part-span flaps increase lift in two different ways:

- They generate and carry lift, or circulation, by themselves
- They generate additional circulation, through favourable interference, on the part of the main-wing in front of them

As a result there are three regions with a locally high spanwise gradient in the bound circulation (fig.3):

- at the wing tip, as usual for wings (without winglets)
- at the tip of the flap
- on the main wing at the spanwise location of the flap tip

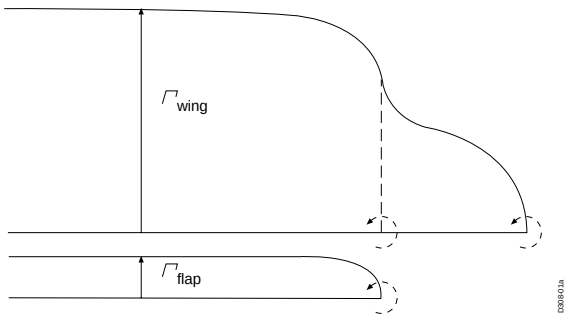

Fig. 3 Span distribution of circulation of a wing with part-span trailing-edge flap (schematic)

These high spanwise gradients in circulation give rise to concentrated trailing vorticity ('trailing vortices') in these regions.
The trailing vortices cause down- and/or upwash on the wing and the flap. This is the mechanism for induced drag. The (locally) induced drag is proportional to the product of downwash and circulation:

$$D_i(y) \propto \Gamma(y) * \alpha_i(y)$$

The local induced drag in a wing section is positive in case the circulation/lift Γ in the section is positive and it is subjected to downwash ($\alpha_i > 0$). The wing tip vortex induces downwash on all of the wing and the flap. The flap tip vortex and flap-tip-induced vortex of the main wing cause downwash inboard of the flap tip and upwash outboard of the flap tip; because of the higher lift/circulation inboard of the flap tip and the larger spanwise extent of the flapped part of the wing their net effect is additional induced drag.
Because the downwash induced by a trailing vortex is inversely proportional to the distance from the trailing vortex, its magnitude can be reduced by moving the trailing vortices out of the plane of, that is farther away from, the wing. This, in essence, represents the (induced) drag reducing mechanism of wing tip winglets: for properly designed winglets, i.e. if there is no boundary layer separation in the intersection of wing with winglet(s), the bound circulation of the wing is carried over to the winglet(s) and shed at the tip(s) of the winglet(s) rather than at the wing tip itself (Fig. 4).

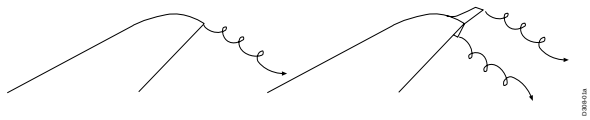

Fig. 4 Illustrating the mechanism of out-of-(wing)plane displacement of the wing tip (trailing) vortex by means of winglets

Although the winglet(s) do experience some induced drag by themselves, this is more than compensated by the reduction of induced drag on the main wing.
Winglets can be applied to either the upper surface or the lower surface of a wing or to both upper and lower surface.
The mechanism, as described, implies that the effectiveness of winglets increases with increasing winglet height/span ratio. It has also been found that the (induced) drag reduction potential of double (upper + lower) winglets is slightly larger than for single (upper or lower) ones.

A negative aspect of winglets, in particular for cruise flight conditions, is that they introduce additional friction drag through the added wetted area.

The winglet concept and underlying mechanism, as outlined above, can also be applied to part-span flaps, with a similar potential for induced drag reduction. This is of interest for the second segment climb of an aircraft.
For part-span flaps two different basic types of winglet or 'device' configurations can be distinguished:

- winglet type devices attached to the tip of the flap (figs. 1 and 5a,b)
- 'fence' type devices attached to the main wing at the spanwise location coinciding with the tip of the flap (figs. 2 and 5c,d)

With the first, that is winglets attached to tip of the flap only, only the bound circulation of the flap can be carried over to the winglet(s). With the second, that is a fence type device attached to the main wing, both part of the bound circulation of the main wing as well as the bound circulation of the flap can be carried over to the fence;

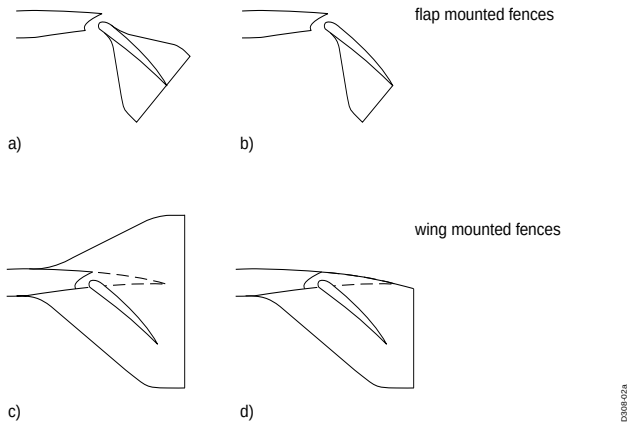

Fig. 5 Illustrating the difference between flap-mounted winglets and wing-mounted fences

provided, of course, that there is no gap between the tip of the flap and fence. This means that, at least in principle, the potential for induced drag reduction is larger for the 'fence' type configuration.

Because the application of winglet as well as fence type devices will change the topology of the trailing vortex system (at least in the near-field, as described above), another interesting aspect is their possible effect on the far-field wake vortex characteristics and the related admissible separation distance between following aircraft. At present it remains to be seen whether this effect will be positive, negative or neutral.

2.2 Acoustics

Pressure fluctuations constitute the basic mechanism for noise generation.
For a part-span trailing-edge flap the flap tip or side edge is the most important noise source. Turbulent pressure and vorticity fluctuations contained by the lower surface boundary layer, separating from the entire (usually sharp) lower side-edge and rolling-up into a concentrated turbulent vortex in close proximity of the sharp side-edges (and, possibly, the sharp trailing-edge of the flap) are believed to form the main mechanism[7,8]. The proximity effect is believed to be caused by unsteady, acoustic 'Kutta-condition' effects at the sharp edges, possibly implying a feed-back and amplification mechanism.
More recently, fluctuations in the turbulent side-edge vortex have been identified as the primary noise source[8,9,10].

It has also been suggested (on a theoretical basis) that the proximity of the undeflected outboard wing panel is important for the radiation characteristics of flap side-edge noise[11]. One might also suspect that the sharp, inboard side-edge of the outer wing panel adjacent to the flap is a noise source by itself, although probably a much weaker one than the flap side-edge because of a much lower aerodynamic loading.
Assuming that the mechanism described above is the correct one, it follows that flap side-edge noise will increase with flap deflection angle, i.e. will be more important for the landing than for the take-off configuration.

The considerations given above suggest that flap tip noise can be reduced by

- reducing the strength of (or eliminating) the flap tip vortex
- avoiding sharp (convex) edges in close proximity of concentrated and (unavoidably) fluctuating vortices

Note that both requirements are fulfilled, in principle, by closing the gap between the tip of the flap and the outboard wing panel.

2.3 Choice of flap tip fence configuration

Based on the mechanisms and following the guidelines established above, the (potential) advantages and disadvantages of the candidate flap tip device configurations distinguished in section 2.1 (fig. 5) can be summarized as follows:

- configuration a):
  - redistributes (carries over) the bound vorticity of the flap to the upper and lower winglets with a good potential for induced drag reduction
  - good potential for noise reduction due to elimination of flap tip vortex, but a gap between flap/winglet and the outer wing panel still exists, as well as the sharp, inboard facing side edge(s) of the aft part of the outer wing panel, adjacent to this gap

  - risk of adverse interaction between the wake of the main-wing and the flow around the upper winglet when the flap is deflected
  - increased complexity of load and structure of the flap (plus winglets) and, possibly, structural interference between the shroud and the winglets
- configuration b):
  - in principle less potential for induced drag reduction than configuration a), since the flap-tip bound vorticity is carried over to a lower winglet only; but on the other hand less additional viscous drag due to a smaller wetted area
  - possibly almost equal potential for noise reduction; some risk of less reduction due to presence of sharp edge on upper side of flap tip
  - avoids the potential problem of configuration a) of adverse interaction between the wake emanating from the main-wing and the upper winglet
- configuration c):
  - anticipates significant concentrated trailing vorticity emanating from the main-wing in the winglet/fence-off configuration and has therefore the largest potential for induced drag reduction
  - probably the best potential for noise reduction due to elimination of the flap tip vortex and elimination of the gap between the deployed flap and outer wing panel
  - relatively high additional viscous drag due to larger wetted area than configuration a)
  - possibly reduced complexity of loads and structure of fences and flap (tip); opportunity for structural integration with flap-track fairings or engine-pylons?
- configuration d):
  - in principle less potential for induced drag reduction due to smaller vertical extension of the fence but still a possibility for some circulation carry-over from main wing; less additional viscous drag due to a smaller wetted area than configuration c)
  - noise reduction potential probably (almost) equal to that of configuration c) since both the flap-tip vortex and the gap between flap and outer wing panel are still avoided

Based on the considerations given above a preference was developed for configurations c) and d).

The precise geometrical dimensions of flap tip devices are, of course, determined by the specifics of the aircraft configuration for which they are intended. In this study this is a (wind tunnel model of a) civil transport type of aircraft configuration equipped with slotted, Fowler-type trailing-edge flaps (slats retracted). Details are provided in the next section.

3 Test set-up

3.1 The model

The wind tunnel model used in this study was the so-called F-29-10-11 (half) model. In the past, this model has been used extensively by the former Fokker Aircraft Company for high-lift configuration studies.

Figure 6 presents a picture of the model as mounted in the wind tunnel.

Fig. 6 The model as mounted in the DNW-LST with acoustic array antenna in side-wall

It is a half model of a port wing with a half-fuselage, without tail planes and, for the present test, also without pylon/nacelle. The main dimensions of the model are: (semi-)span 1.45m, fuselage length 2.7m, fuselage (half) diameter 0.34m.

Figure 7 presents the most important geometrical characteristics of the wing:

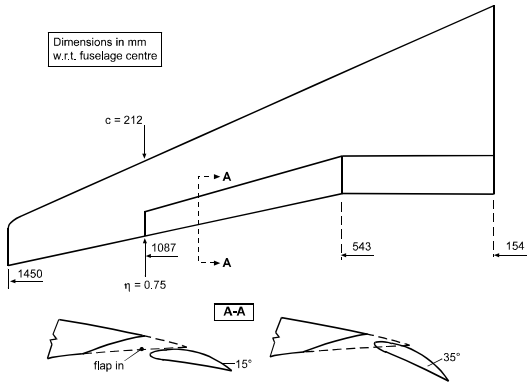

Fig. 7 Main geometrical characteristics of the (wing) configuration represented by the wind tunnel model

Aspect ratio of 9.4, a ¼-chord sweep angle of 22 degrees, 12-15% thick modern ('supercritical') airfoil sections, 75%-span flaps, flap settings 15 degrees for take-off and 35 degrees for the landing configuration. For the present tests the slats were retracted and the flaps were set in their single-slotted configuration.

The model was modified sothat it could be equipped with flap tip fences of the type described in the preceding section. Based on the design considerations given above and the geometrical characteristics of the wind tunnel model, the dimensions of the flap tip fences have been chosen as indicated in fig. 8.

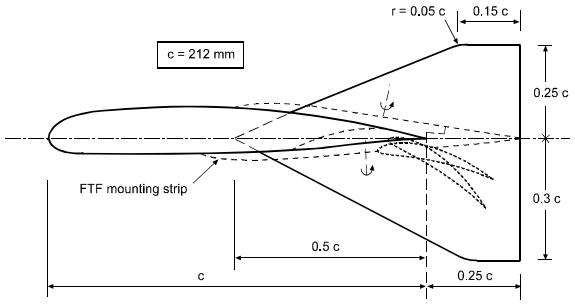

Fig. 8 Main dimensions of the flap tip fences

They imply an increase in wetted area of about 2% of the wing wetted area, corresponding with an estimated increase in friction drag of about 2 'counts' for the double (upper plus lower) and about 1 count for the lower fence only configuration§.
It was decided to partition the upper and lower parts of the fences so that they can be tested separately as well as in combination. Based on the experience of the computational study5 (risk of too much lift, or rather side force and associated leading-edge separation on the fences) it was also decided that it should be possible to vary the angle of (lateral) incidence of the fences between –5 and +5 degrees. Because of the smaller sweep angle of the current configuration (22 degrees versus 30 degrees for the configuration of ref. 5) the risk of leading-edge separation on the fences was considered to be smaller than for the configuration of ref. 5, though.

§ NLR experience suggests that, at cruise conditions, the friction drag penalty may be neutralized by a concurrent reduction of induced drag (See AGARD R-723, Addendum 1, 1985)

The airfoil section chosen for the fences is NACA 63009. This was estimated to be sufficiently thick to avoid early leading-edge separation problems and sufficiently thin to avoid local transonic (shock wave) phenomena in cruise conditions. Optimized sections would probably require some form of twist and camber. This, however, was not pursued at this (exploratory) stage of the investigation.

Figure 9 illustrates some details of the fences as mounted on the model.

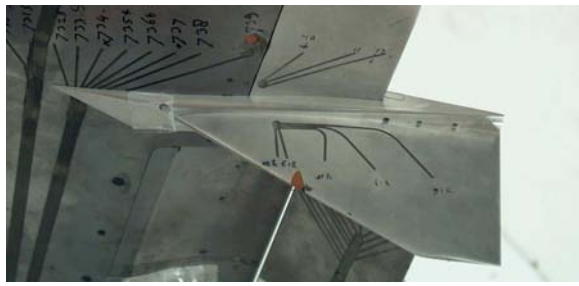

Fig. 9 Details of the flap tip fences as mounted on the model

3.2 The wind tunnel

The tests were done in the LST of the DNW organisation. This is a low-speed, closed circuit type atmospheric wind tunnel with a contraction ratio of 9 and a maximum velocity of 80m/s. The dimensions of the test section are: width 3.0m, height 2.25 meters, length 5.75m.
The model was mounted on a turn table in the lower wall of the test section (Fig. 6) with a 'peniche' of 30mm thickness between the (half) fuselage and the turn table.

3.3 Instrumentation

The following instrumentation was used in the wind tunnel test:

- A five-component half model balance for measuring forces and moments, mounted below the turn table in the lower wall of the tunnel.
- Pressure taps on wing, flap en fences.
- Five-hole probe and PIV measurements for mapping the trailing vorticity in two or three stream-normal planes behind the model
- Tufts and oil for surface flow visualization
- An acoustic array for measuring noise sources

A disadvantage of the balance used is that it has been designed for use in the transonic wind tunnel HST of DNW at much higher absolute force levels. As a consequence only a relatively small part of the range of the balance was used in the present tests, with related consequences for the accuracy of the force measurements, drag in particular. However, by applying statistical

techniques with a number of repeat runs, systematic differences in drag between configurations of more than 2 drag counts could be identified with some (but not absolute) confidence.

The position of the acoustic array, relative to the model, is indicated in figure 10. The array was mounted in the tunnel side wall opposite to the lower surface of the wing. This means that the noise as measured is representative only for fly-over noise at an emission angle of 90 degrees (i.e. directly overhead).

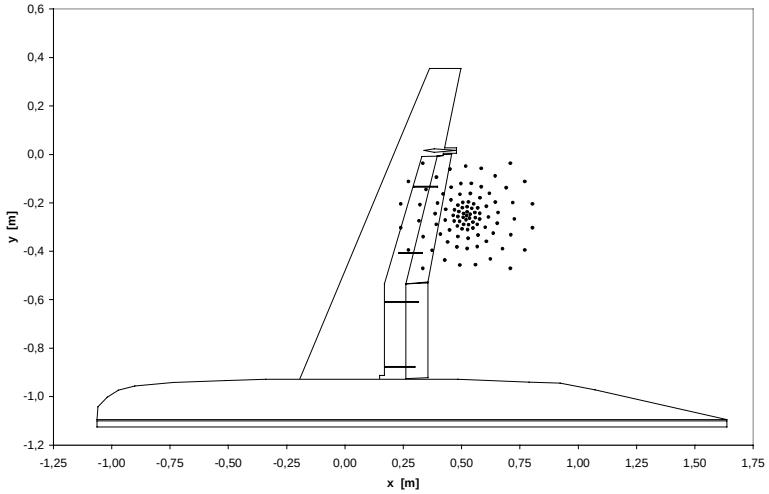

Fig. 10 Position of acoustic antenna

The array contained 96 microphones mounted in a (red) support plate (Fig. 6) covering an area of 57 cm x 44 cm. In order to reduce the effects of reflections and tunnel noise the tunnel wall opposite to the array was fitted with a sound absorbing lining.
The 96 acoustic pressure signals were sampled over a period of 20 seconds with a frequency of 116kHz. From the stored time domain data, a set of monopole sound power values has been calculated on a grid with a spatial resolution of 2 cm, using a conventional beam forming technique, as outlined in ref. 14. Finally, 1/3 octave band sound power levels have been determined covering a frequency range from 50 kHz up to about 4 kHz.

3.4 Test condition

Most of the measurements were done at a tunnel speed of
60 m/s, corresponding with a Mach number of 0.18 and a Reynolds number based on the mean aerodynamic chord of about $1.4*10^6$
In all cases the boundary layer on the wing and on the fuselage was tripped by means of 'zig-zag' tape. On the wing the trip was positioned at 3% of the local chord. On the fuselage the trip was applied near the nose. No tripping was applied on the fences.

Most of the balance measurements were done at a tunnel speed of 60 m/s for an angle of attack range from about -4° till 14° with data collected at 0.25° intervals. For the take-off/climb configuration additional measurements were done at 75 m/s.

PIV measurements were done at 60 m/s; for take-off/climb configurations at an angle of attack of about 5°, corresponding with 0.7 C_{Lmax} ; for approach/landing configurations at an angle of attack of about 0°, corresponding with 0.6 C_{Lmax}.

Five-hole probe measurements were done only for take-off/climb configurations at 0.7 C_{Lmax} , at 60 m/s. Surface oil flow visualisations were obtained for this configuration only.

Acoustic measurements were done only for approach/landing configurations with and without flap tip fences at C_L = 0.6 C_{Lmax} , at both 60 and 75 m/s tunnel speed.

4 Presentation and discussion of results

The presentation and discussion of results given below is limited to the configurations with flap tip fences set at zero lateral incidence. The reasons for this are:

- a(n) (approximately) zero lateral incidence of the flap tip fences is to be preferred in order to minimise any additional drag in cruise conditions
- Pressure distributions measured on the flap tip fences (in qualitative agreement with expectations) and flow visualisation indicated that the fences did not suffer from leading edge separation, the risk of which was suggested in ref. 5 for a configuration with higher wing sweep.
- It was found that changing the lateral angle of incidence of the flap tip fences changed the loading on the fences as expected, but did not seem to have a large effect on the results in terms of aerodynamic forces and wake vortex characteristics

Results are given below for two flap tip fence configurations; lower-fence-only and lower-plus-upper fence, for take-off/climb as well as approach/landing flap settings. They are compared with results for the corresponding configurations without flap tip fences.

4.1 Aerodynamic forces

For the three **take-off/climb** configurations a comparison of lift and drag curves, measured at 75 m/s, is presented in figs 11 and 12.

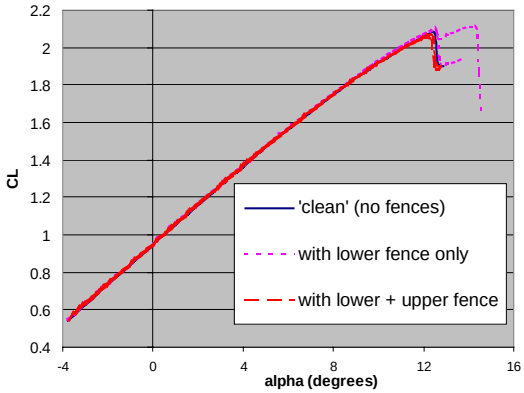

Fig. 11 (a) CL-alpha for the take-off/climb configuration (flap deflection 15 degrees)

As can be observed from fig. 11 the fences have, as expected, only a small effect on lift. At low and moderate angles of attack there is a small and approximately equal increase of lift for both flap tip fence configurations ($\Delta CL \approx 0.01$, not visible on the scale of fig. 11 (a)), increasing (see fig. 11 (b))

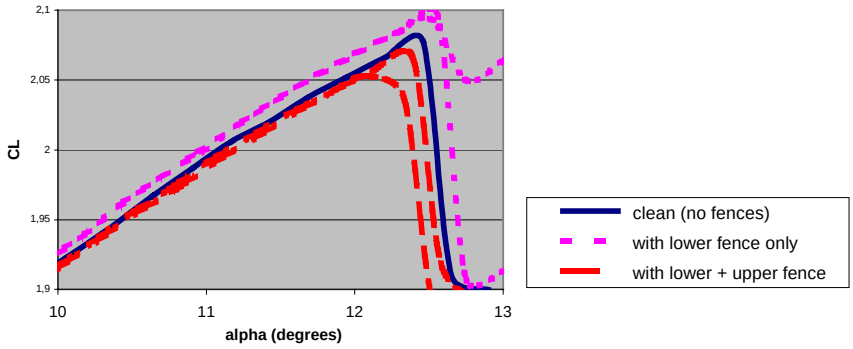

Fig 11 (b) CL-alpha for the take-off/climb configurations (zoom-in near Clmax)

to about $\Delta C_L \approx 0.02$ at C_{Lmax} for the configuration with lower fence only and decreasing to about $\Delta C_L \approx -0.02$ near C_{Lmax} for the configuration with lower-plus-upper fence.

Drag curves are compared in fig. 12.

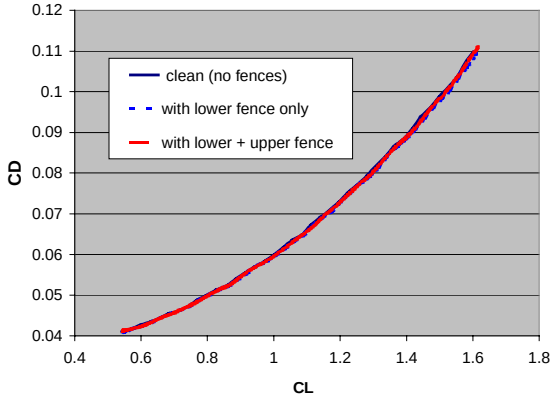

Fig. 12 (a) Drag versus lift for the take-off/climb configuration (flap deflection 15 degrees)

On the scale of fig. 12 (a) differences in drag are hardly visible, in particular at low C_L. The picture is also somewhat obscured by an (approximately) 3 counts scatter in the data, caused by the limited accuracy of the balance.
Systematic differences become apparent if the data are smoothed by a least square quadratic fit. Zooming-in at around $C_L = 0.7*C_{Lmax} \approx 1.4$ it is then found, fig. 12 (b),

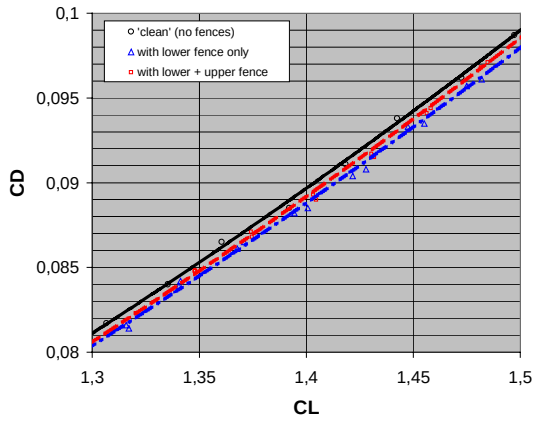

Fig. 12 (b) Drag versus lift for the take-off/climb configuration (zoom-in around $0.7C_{Lmax}$)

that with only the lower fence present there is a drag reduction at $C_L = 0.7*C_{Lmax}$ of about 9 counts. With both lower and upper fence present this is only about 4 counts. Since the (minimum) viscous drag of the configurations with fences must be higher due to added wetted surface (by at least 1 count for the lower fence and at least 2 counts for the lower-plus-upper fences), the drag-due-to-lift is reduced by at least 10 counts for the lower fence only and by at least 6 counts for the lower-plus-upper fence. It is noted that this of the same order of magnitude as found in the numerical simulation of ref. 5.
It is also found that with the lower fence only the drag reduction increases slightly with increasing lift. For the configuration with lower plus upper fence the trend is opposite: the (small) drag reduction appears to decrease with increasing C_L and to increase slightly for lower values of C_L.
The most likely explanation for the lift and drag phenomena described above is that, as intended, both fence configurations do indeed reduce the induced drag, but that the lower-plus-upper fence configuration suffers from additional viscous losses that worsen progressively with increasing angle of attack. Because, as compared with the lower-fence-only configuration, the lift of the upper-plus-lower fence configuration is lower and its drag is higher, at least at high angles of attack, these additional viscous losses must have their origin on the upper surface of the wing. Presumably, they are caused by adverse, viscous interaction between the heavily loaded boundary layer on the upper surface of the wing and the upper fence.

For the **approach/landing** configurations the lift characteristics (fig. 13) are similar to those of the take-off/climb configurations, but there is, of course, a higher level of C_{Lmax}.

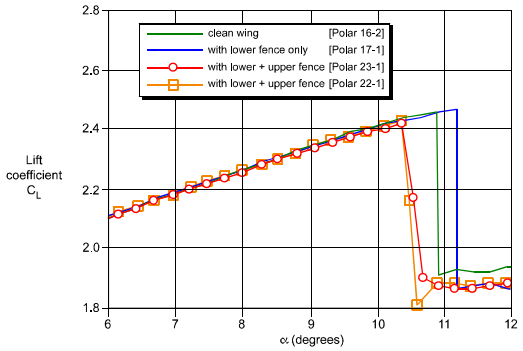

Fig. 13 C_L-alpha for the approach configuration, flap deflection 35 degrees (zoom-in near C_{Lmax})

With only the lower fence present there is a marginal increase of about $\Delta C_L \approx 0.01$ near C_{Lmax}. With both upper and lower fences present there is a small decrease of about $\Delta C_L \approx - 0.02$ of C_{Lmax}. This is (qualitatively) consistent with a picture of increased, adverse interaction between the boundary layer on the upper surface of the wing and the upper fence.

The differences in drag measured for the landing/approach configurations are not significant (< 10 counts) and are therefore not discussed in any further detail.

Differences in pitching moment coefficients were also insignificant ($|\Delta C_M| < 0.003$, that is less than 2%), both for the take-off/climb and the approach/landing configurations and do not need any further discussion either.

4.2 (Near-) wake vortex characteristics

The wake vortex characteristics of the take-off/climb configurations as determined by means of 5-hole probe traverses are depicted in fig. 14. Mappings of the cross-flow velocity vector field and colour-coded distributions of the density of the streamwise vorticity ω_x , where

$\omega_x = \partial v/\partial z - \partial w/\partial y$,

are compared in a free-stream-normal plane located at about 2 local chord lengths downstream of the trailing-edge of the 75% span station. For the configuration with both upper and lower fence the results of an additional traverse at about 0.8 chord behind the 75% span station are also given.

The ‘clean’ (no fences) configuration exhibits the usual pattern of a strong wing tip vortex (in the far left of the picture) and a (slightly less strong) flap tip vortex (in the centre of the picture at y ≈ 0.00, corresponding with 75% semi-span). The third, much weaker vortex, ‘south-south-east’ of the centre, was found to be caused by a flap bracket that, apparently, was not properly aligned with the flow. This ‘flap bracket’ vortex, present for all configurations, is not of interest for the present investigation and is therefore disregarded in the further discussions.
For the configurations with flap tip fences the wing tip and flap bracket vortices are equally identifiable, but the vortex topology around the 75% span station is clearly different and more complex. We will first discuss the pattern for the upper-plus-lower fence configuration for which data from the second wake cut at 0.8 chord downsstream of the 75% semi-span station are also available.

The pictures for the lower-plus-upper fence configuration suggest the presence of three vortices around 75% semi-span: two fairly strong ones and a much weaker one somewhere in-between. Extrapolating their positions upstream towards the trailing-edge of the wing suggests that the two stronger vortices have their origin at the tips of the upper and lower fences, respectively. This, including their sense of rotation, was indeed intended to happen. The third, much weaker vortex, somewhat in-between the two ‘fence tip’ vortices, seems to stem from one, or several, of the intersection(s) of the fence(s) with the flap and/or the main wing.
It is also clear from the wake pictures that the two fence tip vortices are rotating rapidly in a clock-wise direction around a centre that is close to the third, ‘intersection’, vortex.

Turning to the configuration with lower fence only we first of all note that in this case there are two vortices around 75% semi-span. Qualitatively, the picture conforms to expectations, including the sense of rotation of the vortices. The stronger vortex on the left can be retraced to the lower tip of the fence. The weaker one on the right seems to stem from either the upper edge of the fence or the intersection of the flap with the fence.

For the approach/landing configurations wake surveys have been made by PIV only at a condition representative for approach ($C_L \approx 0.6\ C_{Lmax}$). A comparitive summary of cross-flow velocity mappings obtained in three different planes downstream of the model is presented in fig. 15. Note that these pictures cover only a relatively small area around the 75% semi-span station; the wing tip vortex and the ‘flap bracket vortex’ are outside this area.
In a broad sense, the vortex patterns around 75% semi-span appear to be similar to those of the take-off configuration. However, there are some notable differences in details of the vortex topology in the plane nearest to the wing for the configurations with flap tip fence(s). The picture for the lower-fence-only configuration, in the plane at 2 chords behind the wing, suggests the presence of two vortices (like in the take-off/climb configuration), that are

connected by a shear layer. The relative position of these vortices is different, however. Assuming that the origin of these vortices is the same as for the take-off/climb configuration(i.e. one from the lower tip of the fence and one from the top edge of the fence and/or the intersection of the fence with the flap) this means that the two vortices must have rotated around each other by some 180 degrees, instead of the approximately 100 degrees that can be observed in fig. 14 for the take-off/climb configuration. Apparently, they wrap around each other at a faster rate than in take-off/climb. This would mean that the vortices are stronger than in take-off/climb, which, of course, is to be expected because of the larger flap setting and loading in approach/landing.

It can also be noted that, farther downstream, the two vortices merge into a single vortex, leading to a picture that is, qualitatively, quite similar to that for the configuration without flap tip fences.

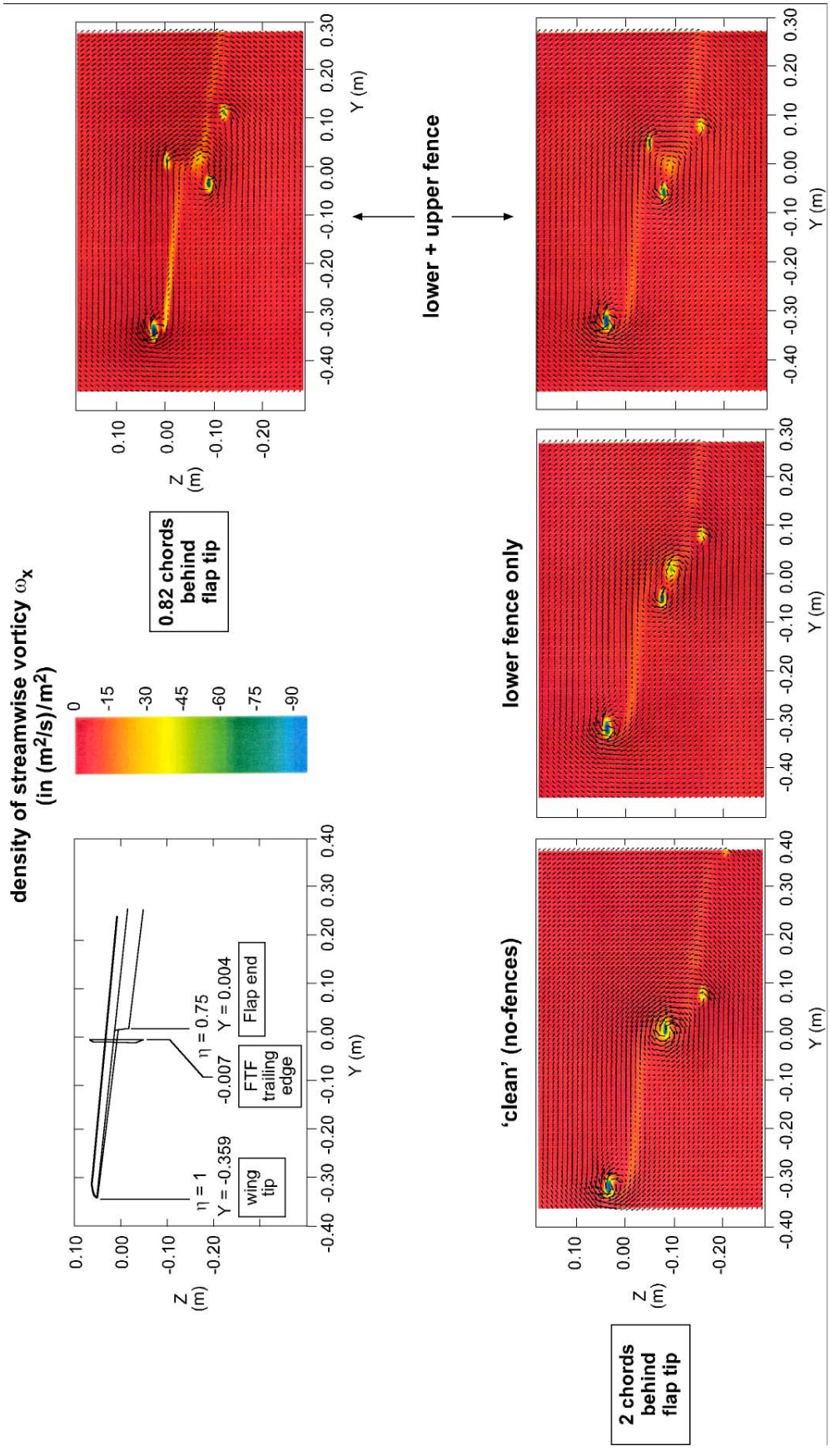

Fig. 14 Wake vortex characteristics as measured by means of 5-hole probe at take-off/climb conditions

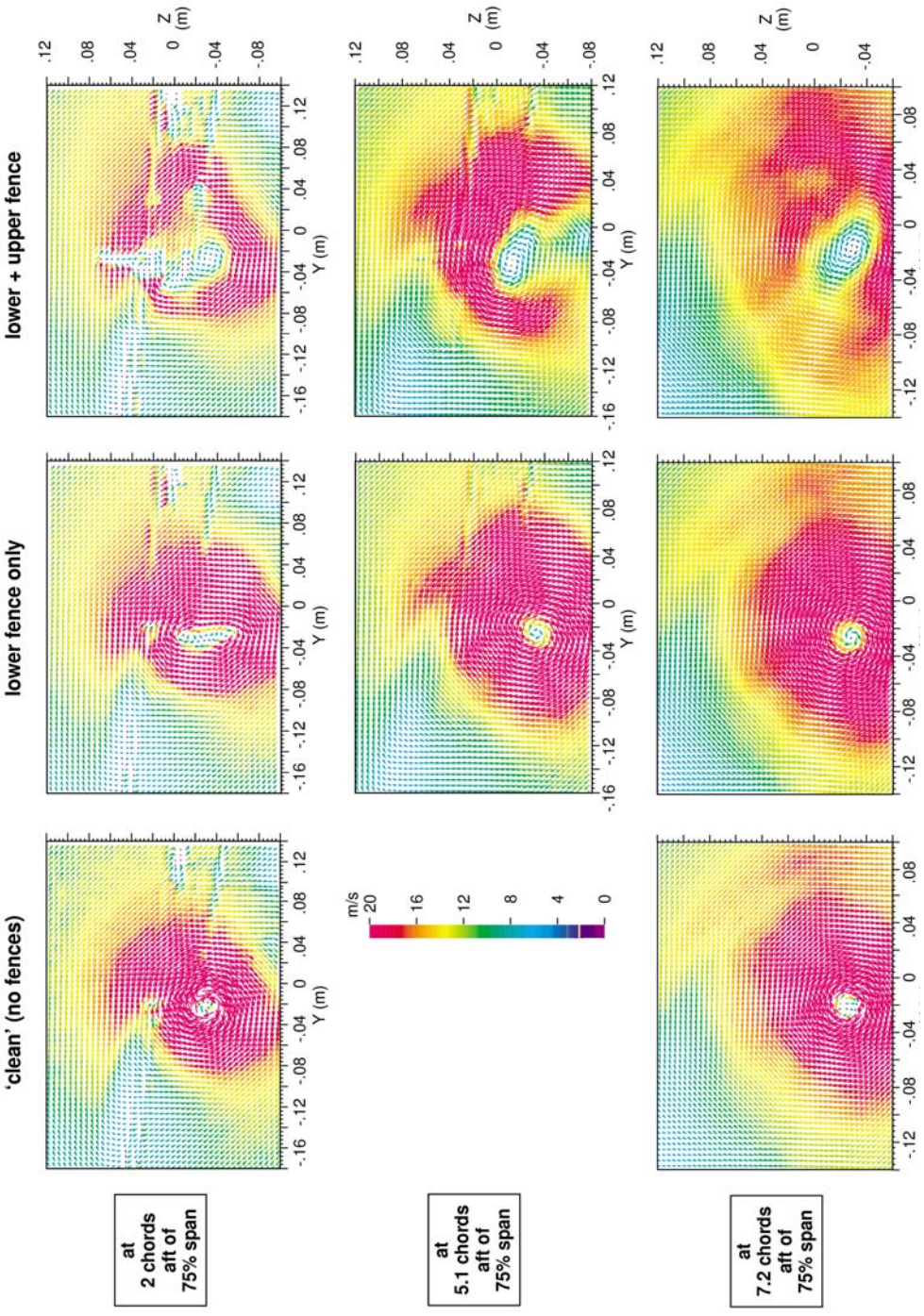

Fig. 15 Comparison of trailing vortex structures from PIV measurements around 75% semi-span for approach conditions

For the approach/landing configuration with both lower plus upper fence the picture at 2 chords behind the wing is more complex (and more fuzzy) than in the case of take-off/climb. What is clear, however, is that, farther downstream, the two or three vortices that seem to be present, merge into a single vortex like in the case of the configuration with lower fence only.

Quantitatively, it is hardly possible to draw conclusions because of the limited accuracy of the PIV measurements. As indicated in the PIV pictures at 7.2 chords downstream in fig. 15, the strength of the trailing vortex from the flap region, in terms of the total amount of circulation Γ contained by the area covered by the PIV measurements, seems to be between 0 and 6 % less when the flap tip fences are present is. The (tentative) conclusion that proposes itself from the wake measurements is that the flap tip fences modify the (near-wake) trailing vortex structure in a qualitative sense, but that, at 7.2 chords downstream, the strength of the trailing vortex from the flap tip area is only marginally smaller.

4.3 Aero-acoustic properties

The main results of the acoustic measurements are presented in figs. 16 and 17.

First of all it is recalled from section 3.3 that the acoustic array technique allows the identification and quantification of the noise sources on the wing under the assumption that the noise sources are of the monopole type, i.e. directivity is not accounted for; the results are representative only for fly-over noise at an emission angle of 90 degrees (i.e. directly overhead). Fig. 16 gives an example of a comparison of the noise source distributions as determined for the indicated configurations without and with flap tip fence(s).

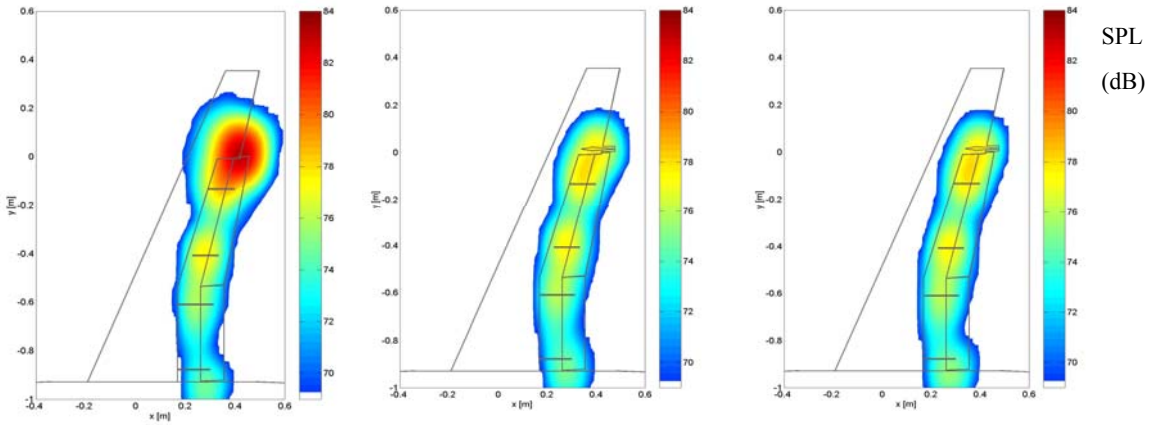

a) without flap tipfence(s) b) with upper +lower fence c) with lower fence only

Fig. 16 Comparison of airframe noise source distributions at approach conditions (8 kHz 1/3 octave band, tunnel speed 75 m/sec)

Presented is the noise source distribution on the model for the 1/3 octave band of 8 kHz and a tunnel speed of 75 m/s. The (local) noise source distribution is given in terms of the sound power level L_w, expressed in decibels:

$$L_w = 10 \log (P/P_{ref}), \quad dB,$$

where P is the sound power in Watt and P_{ref} the reference sound power (10^{-12} W). By definition the sound power P equals the integral of the normal component of the sound intensity over a closed surface around the source.
Figure 16 illustrates clearly that for the 'clean' configuration, that is without flap tip fences, the dominant noise source is located near the tip of the flap. Two or three other, much weaker sources appear to be associated with the flap brackets of the wind tunnel model.
The results also show that with the flap tip fences present the dominant noise source in the region around the tip of the flap has almost dissapeared. For both the lower-fence-only and the lower-plus-upper fence configuration the strength of the dominant source is reduced from about 83 dB to about 78 dB. This suggests that it is the lower fence in particular that is instrumental in reducing flap tip noise.

Fig. 17 presents the reduction of the noise source strength caused by the application of the flap tip fences as a function of the frequency for two wind tunnel speeds (60 m/s and 75 m/s).
For each 1/3 octave band the sound power level (reduction) is assumed to be equal to (the reduction of) the maximum sound power level in the domain
0.23 m $\leq$ x $\leq$ 0.43 m and - 0.1 m $\leq$ y $\leq$ 0.1 m around the flap tip (see Fig. 16).

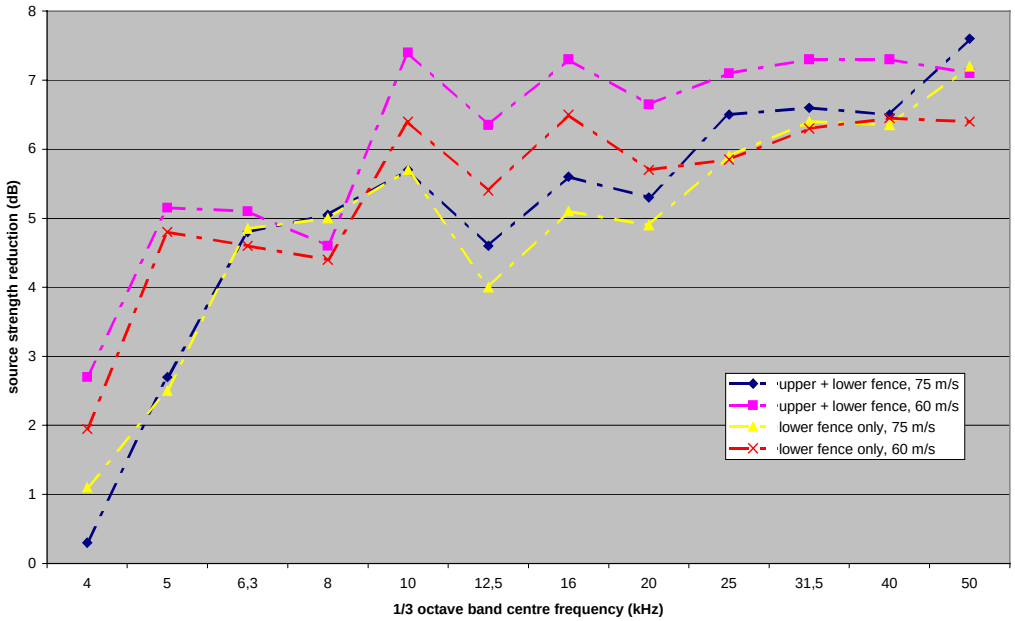

Fig. 17 Airframe noise source reduction, as a function of frequency, as obtained by the application of flap tip fences

It appears that:

- The fences are most effective for frequencies above about 5 kHz (model scale)
- For 60 m/s the noise source reduction (up to about 7 dB) of the lower-plus-upper fence configuration is slightly larger than the reduction (up to about 6 dB) of the lower-fence-only configuration.
- For 75 m/s the difference between the two fence configurations is insignificant.

5 Conclusions

Exploratory, low-speed wind tunnel tests have been performed to investigate the aerodynamic and aero-acoustic effects of winglet type "fences" attached to the main wing of a civil transport type of aircraft configuration at the position of the outboard tip of the trailing-edge flap. Both take-off/climb and approach/landing flap settings were tested.
Two winglet type "fence" configurations have been investigated: a single one extending downward (and rearward) from the lower surface of the wing and a double one extending upward as well as downward from the wing.
The main conclusions from the investigation are that the application of 'flap tip fences' causes:

- a substantial (up to 7 dB) reduction of the noise source level of the flap tip in the approach/landing configuration (about equal for the lower and the upper + lower fence configurations)
- a (small) improvement of L/D and C_{Lmax} in take-off/climb of up to 1% (lower fence only)
- no significant change in pitching moment (less than 2%)
- a noticeable change in the near-field wake vortex topology, resulting however, at 7.2 chords downstream, in a reduction of only a few percent of the strength of the wake vortex from the flap tip region.

6 References

1. J.W. Slooff: Aerodynamic Research for the Next Generation of Commercial Transport Aircraft; The 1994 Jean J. Ginoux Lecture, Von Karman Institute for Fluid Dynamics, Nov. 1994 (unpublished)
2. J.W. Slooff: Subsonic Transport Aircraft – New Challenges and Opportunities for Aerodynamic Research; The 36th Lanchester Lecture, R.Ae.Soc., May 1996 (unpublished)
3. A.C.Willmer, R.V. Barret and J.D. Coleman: The tip flow of a part-span slotted flap; Aeronautical Journal, December 1987
4. J.A. Hayes, W. Clifton Horne, P.T. Soderman an P.H. Bent: Airframe noise characteristics of a 4.7% scale DC-10 model; AIAA paper 97-1595-CP, 1997
5. J.E.J. Maseland and J.W. van der Burg: Numerical investigation of the aerodynamic characteristics of flap tip devices using unstructured grids; NLR-TR-2000-334, 2000
6. A.M.O. Smith: High-lift Aerodynamics, Journal of Aircraft, Vol.12, No.6, 1975
7. D.G.Crighton: Airframe noise, aeroacoustics of flight vehicles: theory and practice; Vol. 1: noise sources; NASA RP 1258, 1991
8. J.C. Hardin: Noise radiation from the side-edges of flaps; AIAA paper 80-4037, 1980
9. M.S. Howe: On the generation of side-edge flap noise; J. Sound and Vibration, Vol.80, No.4, 1982
10. R. Sen: Vortex-Oscillation Model of Airfoil Side-Edge Noise; AIAA J., Vol.35, No.3, March 1997
11. Mehdi R. Khorrami, Bart A. Singer, M.A. Takallu: Analysis of Flap Side-Edge Flowfield for Identification and Modelling of Possible Noise Sources; SAE paper 971917, 1997
12. C.L. Street: Numerical Simulation of a Flap-Edge Flowfield; AIAA 98-2226, 1998
13. Nicolas Molin, Michel Roger: The Use of Amiet's Methods in Predicting the Noise from 2D High-Lift Devices; AIAA-2000-2064, 2000
14. Sijtsma, P., Holthusen, H.: Source location by phased array measurements in closed wind tunnel test sections; AIAA paper 99-1814, 1999